JSR Publications

Available Online

J. Sci. Res. **17** (1), 211-225 (2025)

JOURNAL OF SCIENTIFIC RESEARCH

www.banglajol.info/index.php/JSR

Growth, Spectral, Electrical, Photoluminescence, Thermal, Mechanical and Dielectric Studies of 2-Hydroxy Benzoic Acid (Metabolite of Drug Aspirin) Single Crystal

I. Shubashini (Reg. No. 21111062132003)*, S. R. Jebas

PG and Research Department of Physics, Kamarajar Government Arts College (Affiliated to Manonmaniam Sundaranar University, Abishekapatti) Surandai, Tenkasi Dt, Tamilnadu, India 627859

Received 10 July 2024, accepted in final revised form 12 October 2024

Abstract

2-Hydroxy benzoic acid (2-HBA) is the metabolite of the drug aspirin. The slow evaporation approach was employed to grow the 2-HBA block crystal. Throughout the visible and near-infrared wavelength ranges, the crystal exhibits exceptionally excellent optical transmittance of 99 %. Optical parameters like transmittance, optical absorption coefficient, absorbance, reflectance, optical conductivity, extinction coefficient, refractive index, electrical conductivity, as well as crystal's band gap energy had been computed from UV-Vis-NIR spectrum. From the photoluminescence investigation, violet emission appears at 375 nm. As per the thermogravimetric investigation, the material exhibits stability up to 160 ºC. Vickers microhardness was employed in a mechanical investigation to determine the crystal's elastic stiffness constant, yield strength, as well as work hardening coefficient. Crystal is categorized as a hard material if its work hardening index (n) is less than 2. The Laser damage threshold of 2-HBA crystal is 15.5086 GW/cm^2. This study shows that the 2-HBA crystal exhibits excellent optoelectronics application. The dielectric constant along with dielectric loss is assessed as a function of the frequency.

Keywords: Band gap; Photoluminescence; Thermogravimetric; Mechanical behavior; Elastic stiffness.

doi: https://dx.doi.org/10.3329/jsr.v17i1.74784 J. Sci. Res. **17** (1), 211-225 (2025)

1. Introduction

Nowadays, most of the material science research is intended towards the study of crystals. In an effort to find novel organic crystals for optical applications, numerous studies have been performed over a decade. Development of novel organic materials with desirable features such as a high damage threshold and wide transparency range that allow for frequency doubling has been the focus of much attention in the recent past [1]. To determine whether a material is suitable for optoelectronic applications, it is imperative to study the

* *Corresponding author*: msisuba07@gmail.com

many crystal parameters, transmittance, absorption, refractive index, reflectance, thermal stability, optical conductivity, photoluminescence, electrical conductivity, as well as extinction coefficient [2,3]. The compounds 2-hydroxy benzoic acid (2-HBA) and its derivative are probably two of the best-known instances of aromatic carboxylic acids acting as active mediational compounds. The therapeutic qualities of 2-HBA have been utilized for an extended period. Still, because of the adverse effects, it was substituted with aspirin. Currently, 2-HBA is mostly utilized in chemical synthesis, the food industry, cosmetics, and as a constituent of several co-crystals of pharmacological significance [4]. The optical behavior of the 2-HBA, 3,5 di-isopropyl-2-HBA, 3-hydroxy pyridinium 2-HBA and benzomide 5-chloro-2-HBA has been reported in the literature [5-7]. 2-HBA is widely used in the field of medicine. However, in the literature, there is no study reported about its optical, thermal, electrical and mechanical behavior.

2. Experimental

In order to produce single crystals of superior quality, both organic and inorganic materials have been cultivated utilizing the slow evaporation method. 2-HBA is a white crystalline powder with the chemical formula $C_7H_6O_3$ and a molecular weight of 138.122 g/mol. 5 g of 2-HBA (99 % purity), acquired from ISOCHEM (India), were diluted in 30 mL of acetonitrile without additional purification. The clear, colorless solution was agitated with a magnetic stirrer for one hour at 24 ºC. The clear solution obtained was filtered utilizing Whattman filter paper and the beaker's opening was sealed with silver paper. Minute holes were made on the silver paper to pave slow evaporation of the solution. Colorless block crystals were collected after two weeks. Fig. 1 shows the block crystal of 2-HBA. The chemical diagram of 2-HBA is shown in Fig. 2.

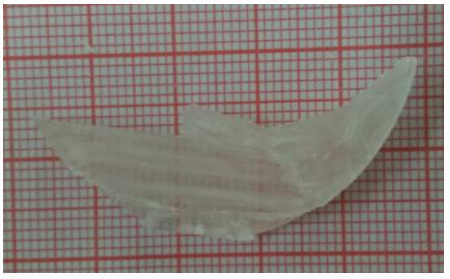

Fig. 1. Photograph of block crystal of 2-HBA.

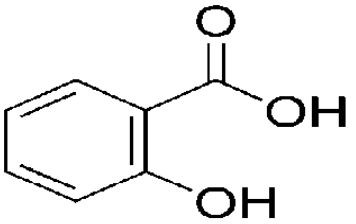

Fig. 2. Molecular structure of 2-HBA.

3. Result and Discussion

3.1. *Fourier transform infrared analysis*

The Fourier transform infrared (FTIR) study entails the analysis of stretching, bending, twisting and vibrational modes of atoms inside a molecule, thus facilitating the

identification of functional groups in crystals. The FTIR spectrum of 2-HBA single crystal was obtained utilizing a Perkin-Elmer FTIR Spectrometer within the region of 4000 cm^{-1} to 400 cm^{-1}. Fig. 3 displays the FTIR spectrum of 2-HBA. The spectrum clearly reveal that the band at 3234 cm^{-1} belongs to the OH asymmetric stretching vibration [8]. The asymmetric as well as symmetric stretching vibrations of aromatic C-H bonds are represented by the absorptions at 3238 and 2988 cm^{-1}, respectively. The C=O vibration of COOH in 2-HBA has a peak at 1620 cm^{-1} [8].

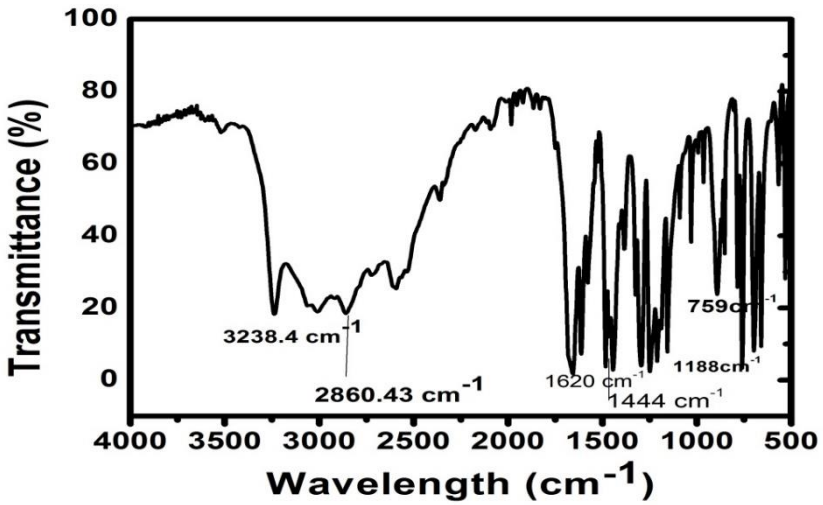

Fig. 3. FTIR spectrum of 2-HBA recorded in KBr pellets.

3.2. *UV-Visible spectral analysis*

Spectrophotometry, commonly referred to as UV-Vis Spectroscopy, is a quantitative technique for assessing the extent of light absorption by a chemical substance. This is achieved by contrasting the light intensity transmitted through a sample with that of a blank or reference sample.

3.2.1. *UV Vis NIR transmission studies*

Utilizing a Perkin Elmer Lambda 35 Spectrophotometer, the UV-Visible NIR transmittance and 2-HBA single crystal absorbance spectrum were captured in the wavelength range of 190 nm to 1100 nm. Figs. 4 and 5 display the spectrums of transmittance as well as absorption. The cutoff wavelength is identified at 380 nm in UV-Vis-NIR spectrum, and the crystal demonstrates excellent transparency of 99 %. Due to π-π^* transitions, the absorption peak was spotted at 380 nm. The low absorption edge is critical for the production of optoelectronic devices.

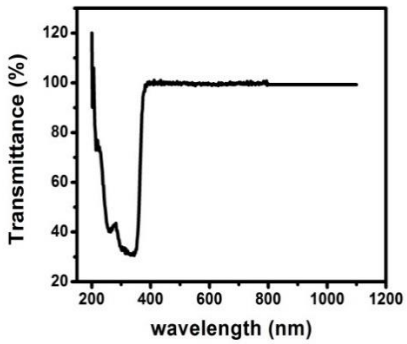

Fig. 4. Optical transmission spectrum of 2-HBA.

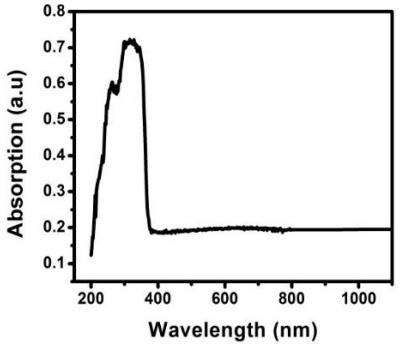

Fig. 5. Optical absorption specrum of 2-HBA.

3.2.2. *Optical band gap energy (E_g) calculation*

For optical device production, the crystal must have exceptional transparency across an extensive spectrum of wavelengths [9] The optical absorption coefficient (α) has been computed from the transmittance spectra utilizing subsequent equation.

$$\alpha = \frac{2.3036 \log\left(\frac{1}{T}\right)}{d} \quad (1)$$

The transmittance is represented by *T*, while the crystal thickness is denoted by *d*. The absorption coefficient (α) at high photon energies ($h\nu$) follows this connection

$$h\nu = \frac{1240}{\lambda} \quad (2)$$

Utilizing the subsequent equation, the band gap energy had been determined [10].

$$(\alpha h\nu)^2 = A(h\nu - E_g) \quad (3)$$

A represents a constant, while the crystal's optical band gap is represented by E_g. The variation of $(\alpha h\nu)^2$ Vs hν in the fundamental absorption zone is illustrated in Fig. 6. 3.6 eV is the band gap energy.

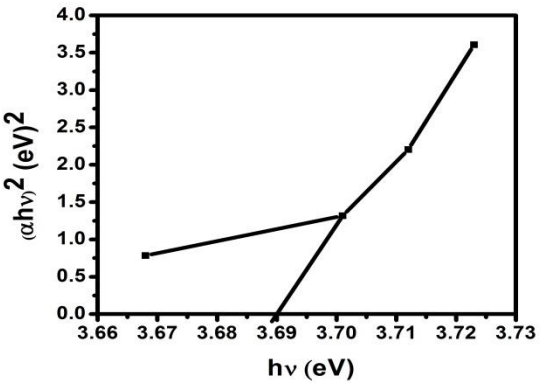

Fig. 6. Variation of hν against $(\alpha h\nu)^2$.

3.2.3. *Optical constants*

The optical characteristics of materials are essential for determining their suitability in the production of optoelectronic devices. The examination of a material's optical constants, that include refractive index as well as extinction coefficient, is crucial for assessing its potential in optoelectronic applications [11]. The optical constants (*n*, *k*) had been obtained from the transmission (*T*) along with reflection (*R*) spectra utilizing subsequent relation.

$$T = \frac{(1-R)^2 \exp(-\alpha t)}{1-R^2 \exp(-2\alpha t)} \quad (4)$$

Where *R* denotes reflectance and *t* signifies thickness. The extinction coefficient (*k*) quantifies the proportion of light loss caused by scattering and absorption per unit distance in a participating medium *T*. The extinction coefficient *K* could be determined through subsequent equation [12].

$$K = \frac{\alpha\lambda}{4\pi} \quad (5)$$

Let α represent the optical absorption coefficient along with λ denote the wavelength. Fig. 7 illustrates the plot of extinction coefficient wavelength v/s wavelength.

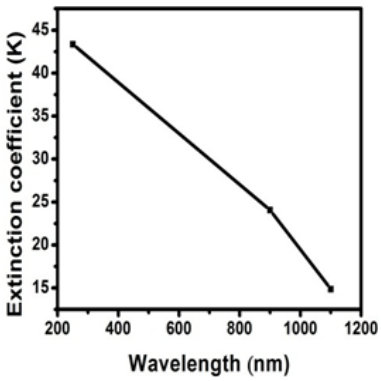

Fig. 7. Variation of wavelength against extinction coefficient.

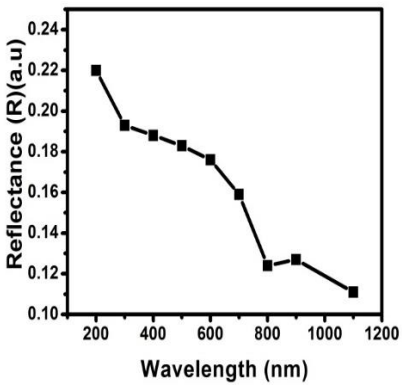

Fig. 8. Variation of wavelength against reflectance.

The reflectance (*R*) denotes the ratio of reflected energy to incident light energy from the crystal. The reflectance *R* can be expressed in relation to the absorption coefficient (α) along with the crystal's thickness (*t*) utilizing the subsequent equation

$$R = 1 \pm \frac{\sqrt{1-\exp(-\alpha t)+\exp(\alpha t)}}{1+\exp(-\alpha t)} \quad (6)$$

Fig. 8 illustrates reflectance as a function of wavelength. The equation can be employed to determine the refractive index n utilizing reflectance data [12].

$$n = \frac{-(R+1)\pm\sqrt{-3R^2+10R-3}}{2(R-1)} \quad (7)$$

The computed refractive index (*n*) for the synthesized 2-HBA crystal, as derived from the above formulae, is 2.51. Fig. 9 illustrates the relationship between wavelength along

with refractive index. The decrease in the material's refractive index with increasing wavelength is a critical parameter for the production of optoelectronic devices.

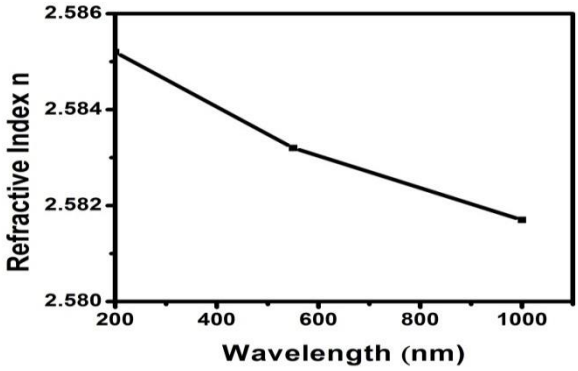

Fig. 9. Plot of wavelength vs refractive index.

3.2.4. *Optical conductivity*

The optical response of a substance is analyzed by its optical conductivity. Optical conductivity serves as a potent instrument for examining the electronic states within materials [13]. The dimensions of frequency are applicable just inside a Gaussian system of units. Based on the relationship, the optical conductivity (σ_{op}) was computed.

$$\sigma_{op}=\alpha nc/4\pi \quad (8)$$

Let the velocity of light has been represented by *c*, α denoting the optical coefficient, as well as n signify the refractive index. Optical conductivity exhibits elevated values in the UV region, of the order of 1×10^{8} S^{-1}.

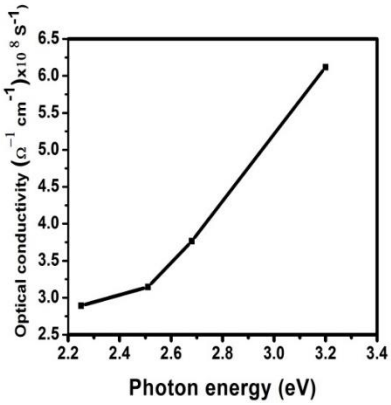

Fig. 10. Change in photon energy with optical conductivity.

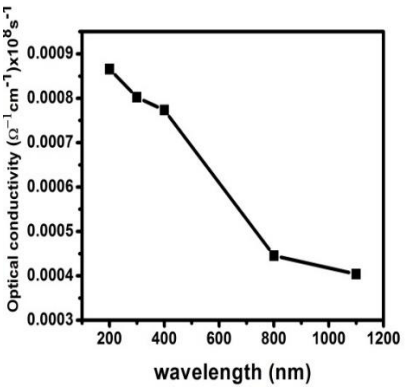

Fig. 11. Change in optical conductivity at different wavelength.

The optical conductivity of 2-HBA rises with increasing photon energy, as illustrated in Fig 10, demonstrating the material's excellent optical responsiveness. Fig. 11 illustrates the variation of optical conductivity with wavelength. The elevated optical conductivity values (10^9-10^{12}) indicate the excellent photo response of the crystals.

3.2.5. *Electrical Conductivity*

The amount of electrical current a substance can conduct is dictated by its electrical conductivity. Equation [14] describes the relationship between a material's electrical conductivity value and the crystal's optical conductivity value. The material's electrical conductivity diminishes as photon energy elevates, as illustrated in Fig. 12

$$\sigma_e = 2\lambda\, \sigma_{op}/\alpha \quad (9)$$

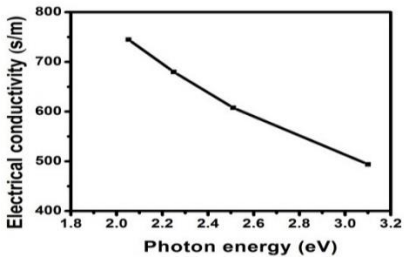

Fig. 12. Variation of photon energy with electrical conductivity

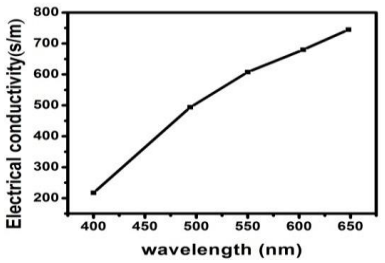

Fig. 13. Change in electrical conductivity at different wavelength.

3.2.6. *Electric susceptibility*

Electric susceptibility is defined as the ratio of polarization (*p*) to the mean electric field (*E*). The electric susceptibility (χc) can be computed through subsequent equation [15]

$$\varepsilon_r = \varepsilon_0 + 4\boldsymbol{\pi}\, \chi_c = \eta^2 - k^2 \quad (10)$$

$$\chi_c = \eta^2 - k^2 - \varepsilon_0/4\boldsymbol{\pi} \quad (11)$$

here the dielectric constant without any free carrier contribution is ε_0. The dielectric constant's real as well as imaginary parts from the extinction coefficient are expressed as εc, which is the complex dielectric constant [16],

$$\varepsilon_c = \varepsilon_r + \varepsilon_i \quad (12)$$

$$\varepsilon_r = n^2 - K^2 \quad (13)$$

$$\varepsilon_i = 2nK \quad (14)$$

here ε_r and ε_i represent the real as well as imaginary components of the dielectric constant, respectively. The electric susceptibility is determined to be $\chi_c = 0.52$.

3.2.7. *Determination of Urbach energy*

The material's linear absorption coefficient (α) is associated with the Urbach energy by the following equation [17]

$$\alpha = \alpha_0 \exp(h\nu/E_u) \quad (15)$$

Here, α_0 represents a constant, and E_u is the Urbach energy, that quantifies the signal depth of tail levels extending into the forbidden electronic band gap beneath the absorption edge. The E_u had been computed as the slope's reciprocal of the plot's linear portion showcasing α against photon energy (hv) illustrated in Fig. 14.

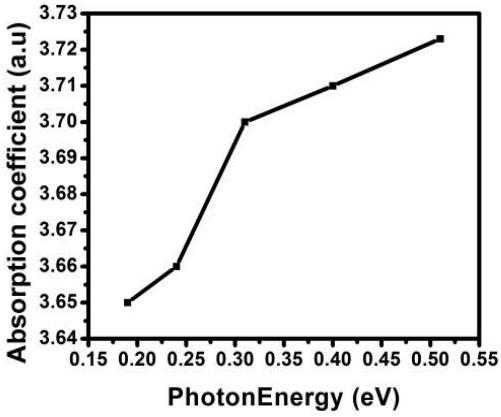

Fig. 14. Plot of photon energy against absorption coefficient

The Urbach energy for 2-HBA crystal has been estimated to be 0.97 eV. This small value indicates that the generated crystal possesses a high degree of crystallinity with few defects at the near band boundaries.

3.2.8. *Determination of steepness parameter (σ_s) and strength of electron phonon interaction*

The ratio of wave height (H) to wavelength (λ) is the steepness parameter. This is crucial as well as a fundamental characteristic that determines how photons and electrons interact. The connection can be used to compute the steepness parameter, that is correlated with Urbach energy along strongly depends on the system's temperature.

$$\sigma_s = K_B T / E_u \quad (17)$$

E_u represents the Urbach energy (0.980 eV), K_B denotes Boltzmann's constant 8.6173 x 10^{-5} eV, as well as T signifies the absolute temperature. The intensity of electron-phonon interaction can be expressed with respect to the steepness parameter.

$$E_{e\text{-}p} = 2/3\ \sigma_s \quad (18)$$

The strength of the electron-phonon interaction is established at 26.67 eV^{-1}, whereas the steepness parameter is assessed to be 0.024 eV. A value of the electron-phonon interaction parameter over 10 is typically regarded as high. The reported crystals, 2-amino-5-methylpyridinium trifluoroacetate, are shown in references [18]. Have an electron-phonon interaction value of 13.58 eV and 0.0491 eV, respectively, for analysis. The compound demonstrates optimal optical density, as seen by the elevated value of the electron-phonon interaction parameter.

3.3. *Photoluminescence analysis*

A prevalent method for characterizing the optical along with electrical characteristics of semiconductors and molecules is Photoluminescence spectroscopy. The method is nondestructive, contactless, as well as rapid. The most commonly used method for identifying vacancies, flaws, and other irregularities in crystals [19] is photoluminescence spectroscopy. This approach elucidates the dynamics of photo-induced electron-hole pair formation, charge separation, and charge recombination processes [20]. At room temperature, photoluminescence experiments were conducted on the crystal within the wavelength range of 300 to 550 nm. The excitation peak is observed at 348 nm. The emission peak had been detected at 375 nm in Fig. 15 indicates that 2-HBA crystal has violet emission. Utilizing the relation 1240 /λ and E_g= 3.31 ev, the crystal's band gap energy had been computed. In this context, *E* represents energy in electron volts (eV), λ denotes wavelength in nanometers (nm), and *v* signifies wave number, measured in cm^{-1}, which is the reciprocal of the wavelength.

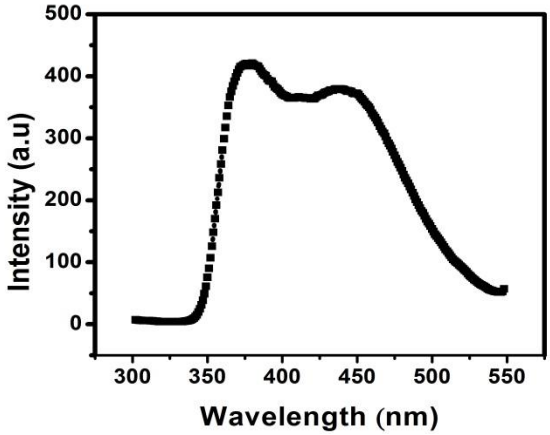

Fig. 15. Photoluminescence spectrum of 2-HBA.

3.4. *Thermal studies*

Thermal analysis is an assessment utilized to investigate the chemical, physical, and structural alterations in a material induced by variations in temperature. Temperature is a fundamental state variable that influences most chemical reactions, physical attributes, and structural transformations.

3.4.1. *TGA/DSC*

A TGA/DSC device is utilized for diagnosing and analyzing phenomena happening in a material under varying thermal temperatures. The TGA (thermal gravimetric analysis)

method quantifies variation in sample mass as a function of temperature or else time in various gaseous atmospheres. Thermal analysis is employed to determine weight loss (TGA) and thermal stability (DSC) of the synthesized crystal in relation to temperature. The TGA curve provides a quantitative assessment of mass variation linked to the transition. The thermal stability of salicylic acid crystals was evaluated utilizing a Perkin-Elmer TGA in conjunction with DSC (Differential Scanning Calorimetry) under an air atmosphere, at a heating rate of 2 ºC/min over 50 ºC to 450 ºC, as illustrated in Fig. 16. The 2-HBA crystal is stable up to 160 ºC and loss in mass is observed on further heating. TGA curve demonstrates single stage weight loss patterns detected from 145 °C up to 225 °C and it is near about 100 % loss of the compound. The sample remains stable up to a temperature of 145 °C as the TGA curve demonstrates, suggesting the material's suitability for optoelectronic applications [21]. The DSC curve reveals the initial endothermic peak at 160 °C, signifying the melting of the crystal, while subsequent endothermic peak at 250 °C confirms the material's decomposition.

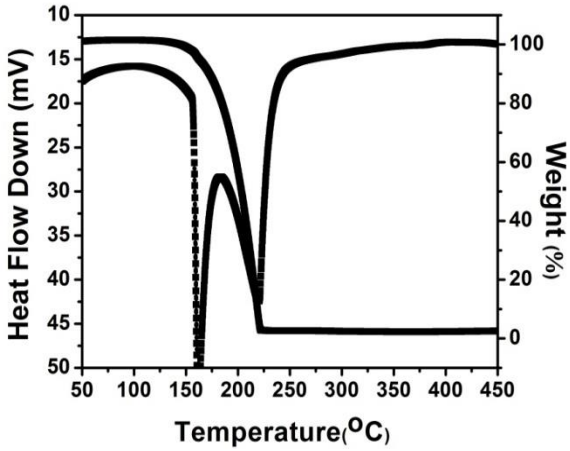

Fig. 16. TGA/DSC curves of 2-HBA.

3.5. *Mechanical studies*

3.5.1. *Micro hardness studies*

To investigate and assess the surface hardness of various materials with Micro-Hardness testing apparatus, specifically the Vicker method. The hardness test is a mechanical evaluation of material qualities utilized in engineering design, structural analysis, and materials development. A diamond pyramid indenter associated with an incident ray research microscope was utilized to conduct a static indentation test, using loads among 10g as well as 100 g to assess the microhardness of the 2-HBA crystal. For every load, an average of three impressions with a dwell period of ten seconds was recorded. Following

unloading, the calibration microscope attached to the system was utilized to measure the indentation mark's diagonal length (*d*). The following formula was used to calculate it.

$H_v=1.8544p/d^2 kg/mm^2$ (19)

The plot of load against hardness is demonstrated in Fig. 17.

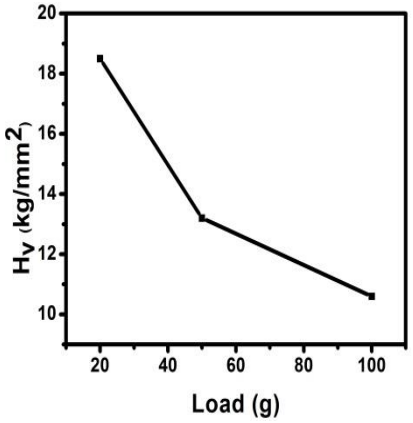

Fig. 17. Plot of load against H_v.

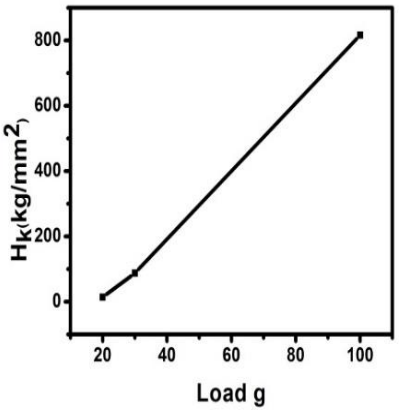

Fig. 18. Plot of load against H_k.

Fig. 17 displays the load vs. hardness value plot. When the load increases, the hardness value decreases, indicating that 2-HBA is exhibiting the typical Indentation size effect (ISE). The indenter only penetrates the crystal's upper surface layer when a modest load is applied, and the hardness value in the low load region decreases based on how the higher layer's strain is distributed [22]. The indenter's depth grows with increasing stress, and the inner and surface layers' combined actions result in a lower hardness rating of thirty. The Knoop intended impressions to be roughly shaped like a rhombohedral. The Knoop micro hardness number H_k was computed utilizing the equation, taking into account average diagonal length (d) [23],

$H_k=14.229p/d^2$ kg /mm^2 (20)

Where H_k is a kg/mm^2, *d* is a mm, along with *p* is the applied load in kg. Mayer's law that establishes a relationship among load as well as indentation diagonal length was used to calculate the Mayer index number.

$np = kd$, $\log p=\log k +\log d$ (21)

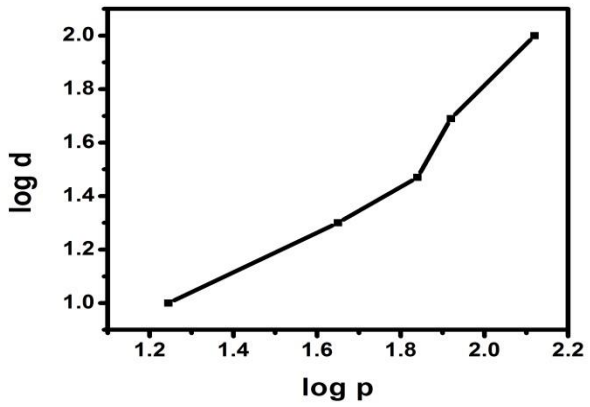

Fig. 19. Plot of log p against log d.

Here *k* is the material constant and *n* is the work hardening coefficient, commonly referred to as Mayer's index. The previously stated relationship suggests that H_v should rise as n increases. The log p as well as log d are plotted to yield the work hardening index (*n*). It turns out that this is 1.416. As stated by Hanneman [24]. The value of *n* is less than two for hard materials. And for soft ones, more than two. 2-HBA crystal falls into the hard material group as a result. The subsequent equation has been utilized to study the strength of the material's yield σ_y.

$$\sigma_y = H_v/3 \quad (22)$$

Elastic stiffness has determined the material's bonding nature. Wooster's expression can be used to compute the material's elastic stiffness constant, C_{11}.

$$C_{11}=H_v^{7/4} \quad (23)$$

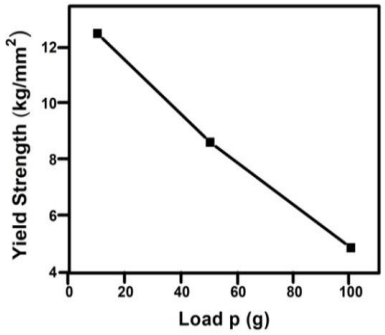

Fig. 20. Load against yield strength.

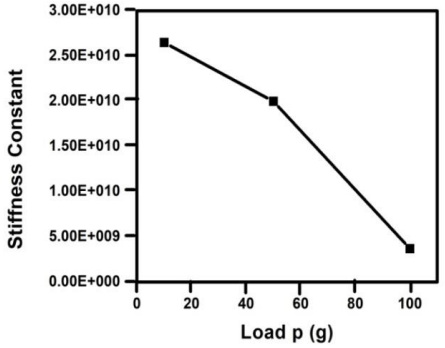

Fig. 21. Plot of load against elastic stiffness.

With increasing load, Figs. 20 and 21 indicate that the yield strength along with elastic stiffness constant of the material improves, suggesting that 2-HBA possesses high mechanical stability based on the above relationship.

3.6. *Laser damage threshold (LDT) studies*

The LDT studies' objective is to determine maximum amount of laser energy a material or optic can withstand before it is permanently damaged. The optical crystal efficiency in LDT research is directly related to basic laser beam power density. A shift in power density causes the optical materials to break down. High energy surface damage resistance is the most crucial characteristic of device manufacture [25]. A material's LDT value is determined by its specific heat and optical absorption. The LDT test was conducted using a flawless and level crystal. When the input laser energy for the KDP (Reference) crystal reached 7.5 mJ, there was evidently damage. Equations were used to estimate the formed crystal's laser damage threshold resistance [26].

$$\text{Power density } P_d = E_p / \tau \pi (\omega_o)^2 \quad (24)$$

Here E_p represents the laser beam input energy (mJ), τ denotes the laser pulse width (ns), and ω_o signifies the beam waist radius at the focal point (cm), ascertained by the subsequent equation:

$$2\,\omega_o = (4\lambda/\pi)\,(f/d) \quad (25)$$

Here, the laser wavelength (1064 nm) is denoted by λ, the convex lens focal length (10 cm) is f as well as the diameter of the laser beam (1 mm) is d. 0.6775 m is the computed value of ω_0. The laser damage threshold value had been observed to be 131 mJ (1.5508 x 10^{-14} W/cm^2) or (15.5086 GW/cm^2). Laser-induced damage in the crystal arises from its optical properties, material defects, impurities, along with surface roughness [27].

3.7. Dielectric *analysis*

The examination of dielectric characteristics pertains to the retention and dissipation of electric as well as magnetic energy within materials. The dielectric studies of 2-HBA crystal have been carried out using Jognic's Model 2816B LCRZ Meter. Figs. 21 and 22 reveal the frequency dependent variations in the dielectric constant along with dielectric loss. It is observed that when the frequency rises, both the dielectric constant and dielectric loss diminish. The elevated dielectric constant values at reduced frequencies result from space charge polarization. The loss of space charge polarizations at elevated frequencies accounts for the reduced dielectric constant at high frequencies [28]. The grown 2-HBA single crystal has good optical quality as the dielectric loss value is small at elevated frequency. This factor is of vital importance for optoelectronics materials [29].

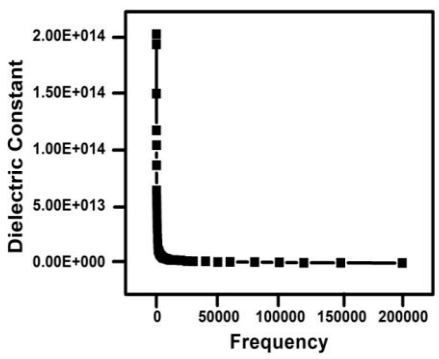

Fig. 22. Plot of frequency against dielectric constant.

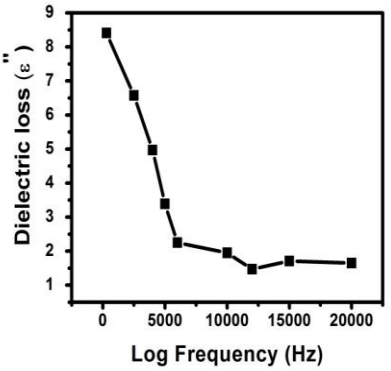

Fig. 23. Plot of Log f against dielectric loss.

4. Conclusion

Single crystal of 2-HBA (metabolite of Aspirin) was cultivated from acetonitrile solvent utilizing the slow evaporation technique. The UV-Visible spectrum was obtained, revealing the wide window transparency of 99 %. The extinction coefficient, refractive index, optical conductivity, susceptibility, electrical conductivity, along with reflectance had been computed as well. TGA/DSC verifies the thermal stability of the crystal up to 160 ºC. Photoluminescence spectral analysis reveals the violet emission of the crystal. The work hardening index (n) of less than 2 represents that the crystal is classified as a hard material. The material's wide band gap, excellent transparency, thermal stability up to 160 ºC, violet emission, and hardness demonstrate its appropriateness for optoelectronic applications. The laser damage threshold is established as 15 GW/cm². This research article confirms, through multiple characterization techniques, that the crystal is suitable for optoelectronic applications.

References

1. H. Nalinia, V. C. Vincenta, G. Bakiyaraj, K. Kirubavathia, and K. Selvaraju, Mol. Cry. Liq. Cry. **712**, 43 (2020). https://doi.org/10.1080/15421406.2020.1856504
2. F. Nekkach, H. Lemziouka, A. Boutahar, R. Moubah, M. El Yazidi, and E. K. Hlil, Opt. Mat. **147**, ID 114686 (2024). https://doi.org/10.1016/j.optmat.2023.114686
3. S. Jin, P. Yan, D. Wang, Y. Xu, Y. Jiang, and L. Hu, J. Mol. Struct. **1016**, 55 (2012). https://doi.org/10.1016/j.molstruc.2012.02.036
4. M. Przybyłek, P. Cysewski, M. Pawelec, D. Ziółkowska, and M. Kobierski, J. Mol. Model. **21**, 49 (2015). https://doi.org/10.1007/s00894-015-2599-z
5. P. Preeda, R. G. Raman, and P. Sakthivel, Inorg Chem. Comm. **146**, ID 110120 (2022). https://doi.org/10.1016/j.inoche.2022.110120
6. K. Anitha, M. Subha, and M. T. Elakkiya, J. Mol. Struct. **1244**, ID 130850 (2021). https://doi.org/10.1016/j.molstruc.2021.130850
7. G. Parvathy, R. Kaliammal, and K. Velsankar, J. Mater. Sci.: Mater. Electron. **33**, 4579 (2022). https://doi.org/10.1007/s10854-021-07649-w

8. A. I. Vogel, A. R. Tatchell, B. S. Furnis, A. J. Hannaford, and P. W. G. Smith, Vogel's Text Book of Practical Organic Chemistry (Longman Scientific & Technical, New York, 1989).
9. S. Panchapakesan, K. Subramani, and B. Srinivasan, J. Mat. Sci: Mate. Elect. **28**, 5754 (2017). https://doi.org/10.1007/s10854-016-6247-x
10. N. Mahalakshmi and M. Parthasarathy, J. Sci. Res. **16**, 449 (2024). https://dx.doi.org/10.3329/jsr.v16i2.67430
11. O. G. Abdullah, S. B. Aziz, and M. A. Rasheed, J. Mate. Sci. Mate Elec. **28**, 4513 (2016). https://doi.org/10.1007/s10854-016-6086-9
12. P. Jayaprakash, P. Sangeetha, C. R. Thayakumarai, and M. Lydiacaroline, Phys. B Con. Mat. **518**, 1 (2017). https://doi.org/10.1016/J.PHYSB.2017.05.017
13. F. D. Selasteen and S. A. C. Raj, Ind. J. Sci. Tech. **14**, 101 (2021). https://doi.org/10.17485/IJST/v14i2.1561
14. T. Murugan, K. S. Murugesan, and B. M. Boaz, Ind. J. Phys. **96**, 3797 (2022). http://dx.doi.org/10.1007/s12648-022-02335-x
15. F. Urbach, Phys. Rev. Atom. Mole. Opt. Phys. **92**, ID 1324 (1953). https://doi.org/10.1103/PhysRev.92.1324
16. A. P. Kochuparampil, J. H. Joshi, and M. J. Joshi, Mod. Phys. Let. B **27**, ID 1750246 (2017). http://dx.doi.org/10.1142/S0217984917502463
17. F. Urbach, Phys. Rev. **92**, 1324 (1953). https://doi.org/10.1103/PhysRev.92.1324
18. S. Kandhan, P. Krishnan, E. Vansu, T. Sahoo, R. Jogan, S. Srinivasan, S. Aravindhan, S. Gunasekaran, and G. Anbalagan, J. Mat. Sci. **55**, 8591 (2020). https://doi.org/10.1007/s10853-020-04575-w
19. Y. Hua, W. Ran, and J. S. Yu, Chem. Eng. **406**, ID 127154 (2021). http://dx.doi.org/10.1016/j.cej.2020.127154
20. S. Sudhakar, M. K. Kumar, A. Silamparasan, and R. Muralidharan, J. Mater. **2013**, 539312 (2013). http://dx.doi.org/10.1155/2013/539312
21. P. G. Jebaraj and V. Sivashankar, J. Adv. Sci. Res. **13**, 54 (2022). http://dx.doi.org/10.55218/JASR.20220000
22. E. M. Onitsh, Uber die Mikroharte der Metalle (Mikroskopie, 1947).
23. C. Chuenarrom, P. Benjakul, and P. Daosodsai, Mat. Res. **12**, 473 (2009) http://dx.doi.org/10.1590/S1516-14392009000400016
24. K Nivetha, S. Kalainathan, M. Yamada, Y. Kondo, and F. Hamada, J. Mater. Chem. Phys. **28,** 5180 (2017). https://doi.org/10.1016/j.matchemphys.2016.12.008
25. P. Karuppusamy, M. S. Pandian, P. Ramasamy, and S. Verma, Opt. Mater. **79**, 152 (2018). https://doi.org/10.1016/j.optmat.2018.03.041
26. R. M. Wood, Laser-induced Damage of Optical Materials (Institute of Physics Publishing, Dirac House, Bristol, UK, 2003)
27. A. Silambarasan, P. Rajesh, , R. Bhatt, I. Bhaumik, A. K. Karnal, P. Ramasamy, and Gupta, App. Phys. A **122**, 736 **(**2016). https://doi.org/10.1007/s00339-016-0255-9
28. P. Karupasamy, M. S. Pandiyan, P. Ramasamy, and S. Verma. Opt. Mat. **79**, 152 (2018). https://doi.org/10.1016/j.optmat.2018.03.041
29. G. P. Smyth, Dielectric Behaviour and Structure (McGraw-Hill, New York, 1955).